EFFICIENT EXPLORATION FOR MODEL-BASED REINFORCEMENT LEARNING WITH CONTINUOUS STATES AND ACTIONS

Anonymous authors
Paper under double-blind review

ABSTRACT

Balancing exploration and exploitation is crucial in reinforcement learning (RL). In this paper, we study the model-based posterior sampling algorithm in continuous state-action spaces theoretically and empirically. First, we improve the regret bound: with the assumption that reward and transition functions can be modeled as Gaussian Processes with linear kernels, we develop a Bayesian regret bound of $\tilde{O}(H^{3/2}d\sqrt{T})$, where H is the episode length, d is the dimension of the state-action space, and T is the time elapsed. Our bound can be extended to nonlinear cases as well: using linear kernels on the feature representation ϕ, the Bayesian regret bound becomes $\tilde{O}(H^{3/2}d_\phi\sqrt{T})$, where d_ϕ is the dimension of the representation space. Moreover, we present MPC-PSRL, a model-based posterior sampling algorithm with model predictive control for action selection. To capture the uncertainty in models and realize posterior sampling, we use Bayesian linear regression on the penultimate layer (the feature representation layer ϕ) of neural networks. Empirical results show that our algorithm achieves the best sample efficiency in benchmark control tasks compared to prior model-based algorithms, and matches the asymptotic performance of model-free algorithms.

1 INTRODUCTION

In reinforcement learning (RL), an agent interacts with an unknown environment which is typically modeled as a Markov Decision Process (MDP). Efficient exploration has been one of the main challenges in RL: the agent is expected to balance between *exploring* unseen state-action pairs to gain more knowledge about the environment, and *exploiting* existing knowledge to optimize rewards in the presence of known data.

To achieve efficient exploration, Bayesian reinforcement learning is proposed, where the MDP itself is treated as a random variable with a prior distribution. This prior distribution of the MDP provides an initial uncertainty estimate of the environment, which generally contains distributions of transition dynamics and reward functions. The epistemic uncertainty (subjective uncertainty due to limited data) in reinforcement learning can be captured by posterior distributions given the data collected by the agent.

Posterior sampling reinforcement learning (PSRL), motivated by Thompson sampling in bandit problems (Thompson, 1933), serves as a provably efficient algorithm under Bayesian settings. In PSRL, the agent maintains a posterior distribution for the MDP and follows an optimal policy with respect to a single MDP sampled from the posterior distribution for interaction in each episode. Appealing results of PSRL in tabular RL were presented by both model-based (Osband et al., 2013; Osband & Van Roy, 2017) and model free approaches (Osband et al., 2019) in terms of the Bayesian regret. For H-horizon episodic RL, PSRL was proved to achieve a regret bound of $\tilde{O}(H\sqrt{SAT})$, where S and A denote the number of states and actions, respectively. But when transferring these results to continous state-action spaces, there could be an exponential growth in dimensionality.

Although PSRL in continuous spaces has also been studied in episodic RL, existing results either provide no guarantee or suffer from an exponential order in term of H. In model-based settings, a bound of $\tilde{O}(\sqrt{d_K d_E T})$ was proved by Osband & Van Roy (2014), where d_K is the Kolmogorov

dimension and d_E is the eluder dimension of the function class. H is not explictly included in the bound, and under their assumptions it can be exponential in H. Moreover, the eluder dimension in general function approximators, such as neural networks, can be presumably huge. Chowdhury & Gopalan (2019) considered kernalized MDPs to further improve the bound with respect to the dimension of d_K and d_E, but H is still unbounded as in Osband & Van Roy (2014). In model-free settings, Azizzadenesheli et al. (2018) developed a regret bound of $\tilde{O}(d_\phi\sqrt{T})$ using a linear function approximator in the Q-network, where d_ϕ is the dimension of the feature representation vector of the state-action space, but their bound can still be exponential in H.

To further imporve the regret bound for PSRL in continuous spaces, especially with explicit dependency on H, we study the model-based posterior sampling algorithm in episodic RL. We assume that rewards and transitions can be modeled as Gaussian Processes with linear kernels, and extend the assumption to non-linear settings that utilize features extracted by neural networks. For the linear case, we develop a Bayesian regret bound of $\tilde{O}(H^{3/2}d\sqrt{T})$. Using feature embedding as mentioned in Yang & Wang (2019), we derive a bound of $\tilde{O}(H^{3/2}d_\phi\sqrt{T})$. Explicitly dependent on d, H, T, our result achieves a significant improvement in terms of the Bayesian regret of PSRL algorithms compared to previous works. Moreover, we implement PSRL using Bayesian linear regression (BLR) on the penultimate layer (for feature representation) of neural networks when fitting transition and reward models. We use model predictive control to optimize the policy under the sampled models in each episode as an approximate solution of the sampled MDP. Experiments show that our algorithm achieves more efficient exploration compare with previous model-based algorithms in control benchmark tasks.

2 Related Work

Besides the aforementioned works on Bayesian regret bounds, the majority of papers in efficient RL choose the non-Bayesian perspective and develop frequentist regret bounds where the regret for any MDP $M^* \in \mathcal{M}$ is bounded and $M^* \in \mathcal{M}$ holds with high probability. frequentist regret bounds can be expressed in the Bayesian view: for a given confidence set $\mathcal{M}$, the frequentist regret bound implies an identical Bayes regret bound for any prior distribution with support on $\mathcal{M}$. Note that frequentist regret is extensively studied in tabular RL (see Jaksch et al. (2010), Azar et al. (2017), and Jin et al. (2018) as examples), among which the best bound for episodic settings is $\tilde{O}(H\sqrt{SAT})$.

There is also a line of work that develops frequentist bounds with feature representation. Most recently, MatrixRL proposed by (Yang & Wang, 2019) uses low dimensional representation and achieves a regret bound of $\tilde{O}(H^2d_\phi\sqrt{T})$, which is the best-known frequentist bound in model based settings. While our method is also model-based, we achieve a tighter regret bound when compared in the Bayesian view. In model-free settings, Jin et al. (2020) developed a bound of $\tilde{O}(H^{3/2}d_\phi^{3/2}\sqrt{T})$. Zanette et al. (2020) further improved the regret to $\tilde{O}(H^{3/2}d_\phi\sqrt{T})$ by the proposed an algorithm called ELEANOR, which achieves the best-known frequentist bound in model-free settings. They showed that it is unimprovable with the help of a lower bound established in the bandit literature. Despite that our regret is developed in model-based settings, it matches their bound with the same order of H, d_ϕ and T in the Bayesian view. Moreover, their algorithm involves optimization over all MDPs in the confidence set, and thus can be computationally prohibitive. Our method is computationally tractable as it can be easily implemented by only optimizing a single sampled MDP, while matching their regret bound in the Bayesian view.

3 Preliminaries

3.1 Problem Formulation

We model an episodic finite-horizon Markov Decision Process (MDP) M as $\{\mathcal{S}, \mathcal{A}, R^M, P^M, H, \sigma_r, \sigma_f, R_{max}, \rho\}$, where $\mathcal{S} \subset \mathbb{R}^{d_s}$ and $\mathcal{A} \subset \mathbb{R}^{d_a}$ denote state and action spaces, respectively. Each episode with length H has an initial state distribution ρ. At time step $i \in [1, H]$ within an episode, the agent observes $s_i \in \mathcal{S}$, selects $a_i \in \mathcal{A}$, receives a noised reward $r_i \sim R^M(s_i, a_i)$ and transitions to a noised new state $s_{i+1} \sim P^M(s_i, a_i)$. More specifically, $r(s_i, a_i) = \bar{r}^M(s_i, a_i) + \epsilon_r$ and $s_{i+1} = f^M(s_i, a_i) + \epsilon_f$, where $\epsilon_r \sim \mathcal{N}(0, \sigma_r^2)$, $\epsilon_f \sim \mathcal{N}(0, \sigma_f^2 I_{d_s})$.

Variances σ_r^2 and σ_f^2 are fixed to control the noise level. Without loss of generality, we assume the expected reward an agent receives at a single step is bounded $|\bar{r}^M(s,a)| \leq R_{max}, \forall s \in \mathcal{S}, a \in \mathcal{A}$,

Let $\mu\colon \mathcal{S} \to \mathcal{A}$ be a deterministic policy. Here we define the value function for state s at time step i with policy μ as $V_{\mu,i}^M(s) = \mathbb{E}[\Sigma_{j=i}^H[\bar{r}^M(s_j,a_j)|s_i = s]$, where $s_{j+1} \sim P^M(s_j,a_j)$ and $a_j = \mu(s_j)$. With the bound expected reward, we have that $|V(s)| \leq HR_{max}, \forall s$.

We use M^* to indicate the real unknown MDP which includes R^* and P^*, and M^* itself is treated as a random variable. Thus, we can treat the real noiseless reward function $\bar{r}^*$ and transition function f^* as random processes as well.

In the posterior sampling algorithm π^{PS}, M^k is a random sample from the posterior distribution of the real unknown MDP M^* in the kth episode, which includes the posterior samples of R^k and P^k , given history prior to the kth episode: $\mathcal{H}_k := \{s_{1,1}, a_{1,1}, r_{1,1}, \cdots, s_{k-1,H}, a_{k-1,H}, r_{k-1,H}\}$, where $s_{k,i}, a_{k,i}$ and $r_{k,i}$ indicate the state, action, and reward at time step i in episode k.

We define the the optimistic policy under M as $\mu^M(s_i) \in_{argmax} V_{\mu,i}^M(s_i)$. In particular, μ^* indicates the optimal policy under M^* and μ^k represents the optimal policy under M^k. Let Δ_k denote the regret over the kth episode:

$$\Delta_k = \int \rho(s_1)(V_{\mu^*,1}^{M^*}(s_1) - V_{\mu^k,1}^{M^*}(s_1))ds_1 \tag{1}$$

Then we can express the regret of π^{ps} up to time step T as:

$$Regret(T, \pi^{ps}, M^*) := \Sigma_{k=1}^{\lceil \frac{T}{H} \rceil} \Delta_k, \tag{2}$$

Let $BayesRegret(T, \pi^{ps}, \phi)$ denote the Beyesian regret of π^{ps} as defined in Osband & Van Roy (2017), where ϕ is the prior distribution of M^*:

$$BayesRegret(T, \pi^{ps}, \phi) = \mathbb{E}[Regret(T, \pi^{ps}, M^*)]. \tag{3}$$

3.2 Assumptions

Generally, we consider modeling an unknown target function $g : \mathbb{R}^d \to \mathbb{R}$. We are given a set of noisy samples $y = [y_1 ...., y_T]^T$ at points $X = [x_1, ..., x_T]^T$, $X \subset D$, where D is compact and convex, $y_i = g(x_i) + \epsilon_i$ with $\epsilon_i \sim N(0, \sigma^2)$ i.i.d. Gaussian noise $\forall i \in \{1, \cdots, T\}$.

We model g as a sample from a Gaussian Process $GP(\mu(x), \mathcal{K}(x, x'))$, specified by the mean function $\mu(x) = \mathbb{E}[g(x)]$ and the covariance (kernel) function $\mathcal{K}(x, x') = \mathbb{E}[(g(x) - \mu(x)(g(x') - \mu(x')]$.

Let the prior distribution without any data as $GP(0, \mathcal{K}(x, x'))$. Then the posterior distribution over g given X and y is also a GP with mean $\mu_T(x)$, covariance $\mathcal{K}_T(x, x')$, and variance $\sigma_T^2(x)$:

$$\begin{aligned} \mu_T(x) &= \mathcal{K}(x, X)(\mathcal{K}(X, X) + \sigma^2 I)^{-1} y \\ \mathcal{K}_T(x, x') &= \mathcal{K}(x, x') - \mathcal{K}(X, x)^T(\mathcal{K}(X, X) + \sigma^2 I)^{-1}\mathcal{K}(X, x) \\ \sigma_T^2(x) &= \mathcal{K}_T(x, x) \end{aligned} \tag{4}$$

where $\mathcal{K}(X, x) = [\mathcal{K}(x_1, x), ..., \mathcal{K}(x_T, x)]^T$, $\mathcal{K}(X, X) = [\mathcal{K}(x_i, x_j)]_{1 \leq i \leq T, 1 \leq j \leq T}$.

We model our reward function $\bar{r}^M$ as a Gaussian Process with noise σ_R^2. For transition models, we treat each dimension independently: each $f_i(s, a), i = 1, .., d_S$ is modeled independently as above, and with the same noise level σ_f^2 in each dimension. Thus it corresponds to our formulation in the RL setting. Since the posterior covariance matrix is only dependent on the input rather than the target value, the distribution of each $f_i(s, a)$ shares the same covariance matrice and only differs in the mean function.

4 Bayesian Regret Analysis

4.1 Linear case

Theorem 1 *In the RL problem formulated in Section 3.1, under the assumption of Section 3.2 with linear kernels, we have $BayesRegret(T, \pi^{ps}, M^*) = \tilde{O}(H^{3/2} d\sqrt{T})$, where d is the dimension of the state-action space, H is the episode length, and T is the time elapsed.*

Proof The regret in episode k can be rearranged as:

$$\Delta_k = \int \rho(s_1)(V^{M^*}_{\mu^*,}(s_1) - V^{M^k}_{\mu^k,1}(s_1)) + (V^{M^k}_{\mu^k,1}(s_1) - V^{M^*}_{\mu^k,1}(s_1)))ds_1 \tag{5}$$

Note that conditioned upon history $\mathcal{H}_k$ for any k, M^k and M^* are identically distributed. Osband & Van Roy (2014) showed that $V^{M^*}_{\mu^*,} - V^{M^k}_{\mu^k,1}$ is zero in expectation, and that only the second part of the regret decomposition need to be bounded when deriving the Bayesian regret of PSRL. Thus we can focus on the policy μ_k, the sampled M^k and real environment data generated by M^*. For clarity, the value function $V^{M^k}_{\mu^k,1}$ is simplified to $V^k_{k,1}$ and $V^{M^*}_{\mu^k,1}$ to $V^*_{k,1}$. It suffices to derive bounds for any initial state s_1 as the regret bound will still hold through integration of the initial distribution $\rho(s_1)$.

We can rewrite the regret from concentration via the Bellman operator (see Section 5.1 in Osband et al. (2013)):

$$\begin{aligned}
&\mathbb{E}[\tilde{\Delta}_k|\mathcal{H}_k] := \mathbb{E}[V^k_{k,1}(s_1) - V^*_{k,1}(s_1)|\mathcal{H}_k] \\
&= \mathbb{E}[\bar{r}^k(s_1,a_1) - \bar{r}^*(s_1,a_1) + \int P^k(s'|s_1,a_1)V^k_{k,2}(s')ds' - \int P^*(s',|s_1,a_1)V^*_{k,2}(s')ds'|\mathcal{H}_k] \\
&= \mathbb{E}[\Sigma^H_{i=1}\bar{r}^k(s_i,a_i) - \bar{r}^*(s_i,a_i) + \Sigma^H_{i=1}(\int (P^k(s'|s_i,a_i) - P^*(s'|s_i,a_i))V^k_{k,i+1}(s')ds')|\mathcal{H}_k] \\
&= \mathbb{E}[\tilde{\Delta}_k(r) + \tilde{\Delta}_k(f)|\mathcal{H}_k]
\end{aligned} \tag{6}$$

where $a_i = \mu_k(s_i), s_{i+1} \sim P^*(s_{i+1}|s_i,a_i), \tilde{\Delta}_k(r) = \Sigma^H_{i=1}\bar{r}^k(s_i,a_i) - \bar{r}^*(s_i,a_i), \tilde{\Delta}_k(f) = \Sigma^H_{i=1}(\int (P^k(s'|s_i,a_i) - P^*(s'|s_i,a_i))V^k_{k,i+1}(s')ds')$. Thus, here (s_i,a_i) is the state-action pair that the agent encounters in the kth episode while using μ_k for interaction in the real MDP M^*. We can define $V_{k,H+1} = 0$ to keep consistency. Note that we cannot treat s_i and a_i as deterministic and only take the expectation directly on random reward and transition functions. Instead, we need to bound the difference using concentration properties of reward and transition functions modeled as Gaussian Processes (which also applies to any state-action pair), and then derive bounds of this expectation. For all i, we have $\int (P^k(s'|s_i,a_i) - P^*(s'|s_i,a_i))V^k_{k,i+1}(s')ds' \leq \max_s |V^k_{k,i+1}(s)| \int |P^k(s'|s_i,a_i) - P^*(s'|s_i,a_i)|ds' \leq HR_{max} \int |P^k(s'|s_i,a_i) - P^*(s'|s_i,a_i)|ds'$.

Lemma 1 *For two multivariate Gaussian distribution $\mathcal{N}(\boldsymbol{\mu}, \sigma^2 I)$, $\mathcal{N}(\boldsymbol{\mu'}, \sigma^2 I)$ with probability density function $p_1(\boldsymbol{x})$ and $p_2(\boldsymbol{x})$ respectively, $\boldsymbol{x} \in \mathbb{R}^d$,*

$$\int |p_1(\boldsymbol{x}) - p_2(\boldsymbol{x})|d\boldsymbol{x} \leq \sqrt{\frac{2}{\pi\sigma^2}}||\boldsymbol{\mu} - \boldsymbol{\mu'}||_2.$$

The proof is in Appendix A.1. Clearly, this result can also be extended to sub-Gaussian noises. Using this lemma, we can derive a regret bound with explicit dependency on the episode length H.

Recall that $P^k(s'|s_i,a_i) = \mathcal{N}(f^k(s_i,a_i), \sigma_f^2 I)$ and $P^*(s'|s_i,a_i) = \mathcal{N}(f^*(s_i,a_i), \sigma_f^2 I)$. By Lemma 1 we have

$$\int |P^k(s'|s_i,a_i) - P^*(s'|s_i,a_i)|ds' \leq \sqrt{\frac{2}{\pi\sigma_f^2}}||f^k(s_i,a_i) - f^*(s_i,a_i)||_2 \tag{7}$$

Lemma 2 *(Rigollet & Hütter, 2015) Let $X_1, ..., X_N$ be N sub-Gaussian random variables with variance σ^2 (not required to be independent). Then for any $t > 0$, $\mathbb{P}(\max_{1\leq i\leq N} |X_i| > t) \leq 2Ne^{-\frac{t^2}{2\sigma^2}}$.*

Given history $\mathcal{H}_k$, let $\bar{f}^k(s,a)$ indicate the posterior mean of $f^k(s,a)$ in episode k, and $\sigma_k^2(s,a)$ denotes the posterior variance of f^k in each dimension. Note that f^* and f^k share the same variance in each dimension given history $\mathcal{H}_k$, as described in Section 3. Consider all dimensions of the state space, by Lemma 2, we have that with probability at least $1-\delta$, $\max_{1\leq i\leq d_s} |f^k_i(s,a) - \bar{f}^k_i(s,a)| \leq \sqrt{2\sigma_k^2(s,a)log\frac{2d_s}{\delta}}$. Also, we can derive an upper bound for the norm of the state

difference $||f^k(s,a) - \bar{f}^k(s,a)||_2 \leq \sqrt{d_s}\max_{1\leq i\leq d_s}|f_i^k(s,a) - \bar{f}_i^k(s,a)|$, and so does $||f^*(s,a) - \bar{f}^k(s,a)||_2$ since f^* and f^k share the same posterior distribution. By the union bound, we have that with probability at least $1-2\delta$ $||f^k(s,a) - f^*(s,a)||_2 \leq 2\sqrt{2d_s\sigma_k^2(s,a)log\frac{2d_s}{\delta}}$.

Then we look at the sum of the differences over horizon H, without requiring each variable in the sum to be independent:

$$\begin{aligned}
&\mathbb{P}(\Sigma_{i=1}^H||f^k(s_i,a_i) - f^*(s_i,a_i)||_2 > \Sigma_{i=1}^H 2\sqrt{2d_s\sigma_k^2(s_i,a_i)log\frac{2d_s}{\delta}}) \\
&\leq \mathbb{P}(\bigcup_{i=1}^H\{||f^k(s_i,a_i) - f^*(s_i,a_i)||_2 > 2\sqrt{2d_s\sigma_k^2(s_i,a_i)log\frac{2d_s}{\delta}}\}) \\
&\leq \Sigma_{i=1}^H\mathbb{P}(||f^k(s_i,a_i) - f^*(s_i,a_i)||_2 > 2\sqrt{2d_s\sigma_k^2(s_i,a_i)log\frac{2d_s}{\delta}})
\end{aligned} \tag{8}$$

Thus, with probability at least $1-2H\delta$, we have $\Sigma_{i=1}^H||f^k(s_i,a_i) - f^*(s_i,a_i)||_2 \leq \Sigma_{i=1}^H 2\sqrt{2d_s\sigma_k^2(s_i,a_i)log\frac{2d_s}{\delta}}$. Let $\delta' = 2H\delta$, we have that with probability $1-\delta$, $\Sigma_{i=1}^H||f^k(s_i,a_i) - f^*(s_i,a_i)||_2 \leq \Sigma_{i=1}^H 2\sqrt{2d_s\sigma_k^2(s_i,a_i)log\frac{4Hd_s}{\delta}} \leq 2H\sqrt{2d_s\sigma_k^2(s_{k_{max}},a_{k_{max}})log\frac{4Hd_s}{\delta}}$, where the index $k_{max} = \arg\max_i \sigma_k(s_i,a_i), i = 1,...,H$ in episode k. Here, since the posterior distribution is only updated every H steps, we have to use data points with the max variance in each episode to bound the result. Similarly, using the union bound for $[\frac{T}{H}]$ episodes, and let $C = \sqrt{\frac{2}{\pi\sigma_f^2}}$, we have that with probability at least $1-\delta$

$$\begin{aligned}
\Sigma_{k=1}^{[\frac{T}{H}]}[\tilde{\Delta}_k(f)|\mathcal{H}_k] &\leq \Sigma_{k=1}^{[\frac{T}{H}]}\Sigma_{i=1}^H 2CHR_{max}||f^k(s_i,a_i) - f^*(s_i,a_i)||_2 \\
&\leq \Sigma_{k=1}^{[\frac{T}{H}]}4CH^2R_{max}\sqrt{2d_s\sigma_k^2(s_{k_{max}},a_{k_{max}})log\frac{4Td_s}{\delta}}
\end{aligned} \tag{9}$$

In each episode k, let $\sigma_k^{'2}(s,a)$ denote the posterior variance given only a subset of data points $\{(s_{1_{max}},a_{1_{max}}),...,(s_{k-1_{max}},a_{k-1_{max}})\}$, where each element has the max variance in the corresponding episode. By Eq.(6) in Williams & Vivarelli (2000), we know that the posterior variance reduces as the number of data points grows. Hence $\forall(s,a), \sigma_k^2(s,a) \leq \sigma_k^{'2}(s,a)$. By Theorem 5 in Srinivas et al. (2012) which provides a bound on the information gain, and Lemma 2 in Russo & Van Roy (2014) that bounds the sum of variances by the information gain, we have that $\Sigma_{k=1}^{[\frac{T}{H}]}\sigma_k^{'2}(s_{k_{max}},a_{k_{max}}) = \mathcal{O}((d_s+d_a)log[\frac{T}{H}])$ for linear kernels with bounded variances. Note that the bounded variance property for linear kernels only requires the range of all state-action pairs actually encountered in M^* not to expand to infinity as T grows, which holds in general episodic MDPs.

Thus with probability $1-\delta$, and let $\delta = \frac{1}{T}$,

$$\begin{aligned}
&\Sigma_{k=1}^{[\frac{T}{H}]}[\tilde{\Delta}_k(f)|\mathcal{H}_k] \leq \Sigma_{k=1}^{[\frac{T}{H}]}4CH^2R_{max}\sqrt{2d_s\sigma_k^2(s_{k_{max}},a_{k_{max}})log\frac{4Td_s}{\delta}} \\
&\leq \Sigma_{k=1}^{[\frac{T}{H}]}8CH^2R_{max}\sqrt{d_s\sigma_k^{'2}(s_{k_{max}},a_{k_{max}})log(2Td_s)} \\
&\leq 8CH^2R_{max}\sqrt{\Sigma_{k=1}^{[\frac{T}{H}]}\sigma_k^{'2}(s_{k_{max}},a_{k_{max}})}\sqrt{[\frac{T}{H}]}\sqrt{d_slog(2Td_s)} \\
&= 8CH^{\frac{3}{2}}R_{max}\sqrt{T}\sqrt{d_slog(2Td_s)} * \sqrt{\mathcal{O}((d_s+d_a)log[\frac{T}{H}])} = \tilde{\mathcal{O}}((d_s+d_a)H^{\frac{3}{2}}\sqrt{T})
\end{aligned} \tag{10}$$

where $\tilde{\mathcal{O}}$ ignores logarithmic factors.

Therefore, $\mathbb{E}[\Sigma_{k=1}^{[\frac{T}{H}]}\tilde{\Delta}_k(f)|\mathcal{H}_k] \leq (1-\frac{1}{T})\tilde{\mathcal{O}}((d_s+s_a)H^{\frac{3}{2}}T) + \frac{1}{T}2HR_{max} * [\frac{T}{H}] = \tilde{\mathcal{O}}(H^{\frac{3}{2}}d\sqrt{T})$, where $2HR_{max}$ is the upper bound on the difference of value functions, and $d = d_s + d_a$. By similar derivation, $\mathbb{E}[\Sigma_{k=1}^{[\frac{T}{H}]}\tilde{\Delta}_k(r)|\mathcal{H}_k] = \tilde{\mathcal{O}}(\sqrt{dHT})$. Finally, through the tower property we have $BayesRegret(T,\pi^{ps},M^*) = \tilde{\mathcal{O}}(H^{\frac{3}{2}}d\sqrt{T})$.

Algorithm 1 MPC-PSRL

Initialize data $\mathcal{D}$ with random actions for one episode
repeat
  Sample a transition model and a cost model at the beginning of each episode
  for $i = 1$ to H steps **do**
    Obtain action using MPC with planning horizon τ: $a_i \in \arg\max_{a_{i:i+\tau}} \sum_{t=i}^{i+\tau} \mathbb{E}[r(s_t, a_t)]$
    $\mathcal{D} = \mathcal{D} \cup \{(s_i, a_i, r_i, s_{i+1})\}$
  end for
  Train cost and dynamics representations ϕ_r and ϕ_f using data in $\mathcal{D}$
  Update $\phi_r(s, a)$, $\phi_f(s, a)$ for all (s, a) collected
  Perform posterior update of w_r and w_f in cost and dynamics models using updated representations $\phi_r(s, a)$, $\phi_f(s, a)$ for all (s, a) collected
until convergence

□

4.2 Nonlinear case via feature representation

We can slightly modify the previous proof to derive the bound in settings that use feature representations. We can transform the state-action pair (s, a) to $\phi_f(s, a) \in \mathbb{R}^{d_\phi}$ as the input of the transition model , and transform the newly transitioned state s' to $\psi_f(s') \in \mathbb{R}^{d_\psi}$ as the target, then the transition model can be established with respect to this feature embedding. We further assume $d_\psi = O(d_\phi)$ as in Yang & Wang (2019). Besides, we assume $d_{\phi'} = O(d_\phi)$ in the feature representation $\phi_r(s, a) \in \mathbb{R}^{d_{\phi'}}$, then the reward model can also be established with respect to the feature embedding. Following similar steps, we can derive a Bayesian regret of $\tilde{O}(H^{3/2} d_\phi \sqrt{T})$.

5 Algorithm Description

In this section, we elaborate our proposed algorithm, MPC-PSRL, as shown in Algorithm 1.

5.1 Predictive model

When model the rewards and transitions, we use features extracted from the penultimate layer of fitted neural networks, and perform Bayesian linear regression on the feature vectors to update posterior distributions.

Feature representation: we first fit neural networks for transitions and rewards, using the same network architecture as Chua et al. (2018). Let x_i denote the state-action pair (s_i, a_i) and y_i denote the target value. Specifically, we use reward r_i as y_i to fit rewards, and we take the difference between two consecutive states $s_{i+1} - s_i$ as y_i to fit transitions. The penultimate layer of fitted neural networks is extracted as the feature representation, denoted as ϕ_f and ϕ_r for transitions and rewards, respectively. Note that in the transition feature embedding, we only use one neural network to extract features of state-action pairs from the penultimate layer to serve as ϕ, and leave the target states without further feature representation (the general setting is discussed in Section 4.2 where feature representations are used for both inputs and outputs), so the dimension of the target in the transition model $d(\psi)$ equals to d_s. Thus we have a modified regret bound of $\tilde{O}(H^{3/2} \sqrt{d d_\phi T})$. We do not find the necessity to further extract feature representations in the target space, as it might introduce additional computational overhead. Although higher dimensionality of the hidden layers might imply better representation, we find that only modifying the width of the penultimate layer to $d_\phi = d_s + s_a$ suffices in our experiments for both reward and transition models. Note that how to optimize the dimension of the penultimate layer for more efficient feature representation deserves further exploration.

Bayesian update and posterior sampling: here we describe the Bayesian update of transition and reward models using extracted features. Recall that Gaussian process with linear kernels is equivalent to Bayesian linear regression. By extracting the penultimate layer as feature representation ϕ, the target value y and the representation $\phi(x)$ could be seen as linearly related: $y = w\top\phi(x) + \epsilon$, where

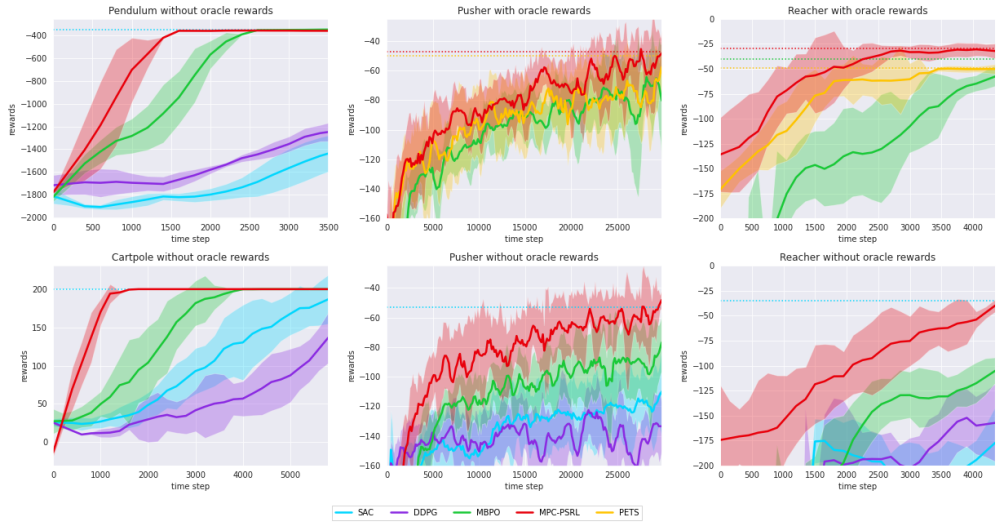

Figure 1: Training curves of MPC-PSRL (shown in red), and other baseline algorithms in different tasks. Solid curves are the mean of five trials, shaded areas correspond to the standard deviation among trials, and the doted line shows the rewards at convergence.

ϵ is a zero-mean Gaussian noise with variance σ^2 (which is σ_f^2 for the transition model and σ_r^2 for the reward model as defined in Section 3.1). We choose the prior distribution of weights w as zero-mean Gaussian with covariance matrix Σ_p, then the posterior distribution of w is also multivariate Gaussian (Rasmussen (2003)):

$$p(w|\mathcal{D}) \sim \mathcal{N}\left(\sigma^{-2}A^{-1}\Phi Y, A^{-1}\right)$$

where $A = \sigma^{-2}\Phi\Phi^\top + \Sigma_p^{-1}$, $\Phi \in \mathcal{R}^{d\times N}$ is the concatenation of feature representations $\{\phi(x_i)\}_{i=1}^N$, and $Y \in \mathcal{R}^N$ is the concatenation of target values. At the beginning of each episode, we sample w from the posterior distribution to build the model, collect new data during the whole episode, and update the posterior distribution of w at the end of the episode using all the data collected.

Besides the posterior distribution of w, the feature representation ϕ is also updated in each episode with new data collected. We adopt a similar dual-update procedure as Riquelme et al. (2018): after representations for rewards and transitions are updated, feature vectors of all state-action pairs collected are re-computed. Then we apply Bayesian update on these feature vectors. See the description of Algorithm 1 for details.

5.2 PLANNING

During interaction with the environment, we use a MPC controller (Camacho & Alba (2013)) for planning. At each time step i, the controller takes state s_i and an action sequence $a_{i:i+\tau} = \{a_i, a_{i+1}, \cdots, a_{i+\tau}\}$ as the input, where τ is the planning horizon. We use transition and reward models to produce the first action a_i of the sequence of optimized actions $\arg\max_{a_{i:i+\tau}} \sum_{t=i}^{i+\tau} \mathbb{E}[r(s_t, a_t)]$, where the expected return of a series of actions can be approximated using the mean return of several particles propagated with noises of our sampled reward and transition models. To compute the optimal action sequence, we use CEM (Botev et al. (2013)), which samples actions from a distribution closer to previous action samples with high rewards.

6 EXPERIMENTS

We compare our method with the following state-of-the art model-based and model-free algorithms on benchmark control tasks.

Model-free: Soft Actor Critic (SAC) from Haarnoja et al. (2018) is an off-policy deep actor-critic algorithm that utilizes entropy maximization to guide exploration. Deep Deterministic Policy Gradient

(DDPG) from Barth-Maron et al. (2018) is an off-policy algorithm that concurrently learns a Q-function and a policy, with a discount factor to guide exploration.

Model-based: Probabilistic Ensembles with Trajectory Sampling (PETS) from Chua et al. (2018) models the dynamics via an ensemble of probabilistic neural networks to capture epistemic uncertainty for exploration, and uses MPC for action selection, with a requirement to have access to oracle rewards for planning. Model-Based Poilcy Optimization (MBPO) from Janner et al. (2019) uses the same bootstrap ensemble techniques as PETS in modeling, but differs from PETS in policy optimization with a large amount of short model-generated rollouts, and can cope with environments with no oracle rewards provided. We do not compare with Gal et al. (2016), which adopts a single Bayesian neural network (BNN) with moment matching, as it is outperformed by PETS that uses an ensemble of BNNs with trajectory sampling. And we don't compare with GP-based trajectory optimization methods with real rewards provided (Deisenroth & Rasmussen, 2011; Kamthe & Deisenroth, 2018), which are not only outperformed by PETS, but also computationally expensive and thus are limited to very small state-action spaces.

We use environments with various complexity and dimensionality for evaluation. Low-dimensional environments: continuous Cartpole ($d_s = 4$, $d_a = 1, H = 200$, with a continuous action space compared to the classic Cartpole, which makes it harder to learn) and Pendulum Swing Up ($d_s = 3$, $d_a = 1, H = 200$, a modified version of Pendulum where we limit the start state to make it harder for exploration). Trajectory optimization with oracle rewards in these two environments is easy and there is almost no difference in the performances for all model-based algorithms we compare, so we omit showing these learning curves. Higher dimensional environments: 7-DOF Reacher ($d_s = 17, d_a = 7, H = 150$) and 7-DOF pusher ($d_s = 20, d_a = 7, H = 150$) are two more challenging tasks as provided in Chua et al. (2018), where we conduct experiments both with and without true rewards, to compare with all baseline algorithms mentioned.

The learning curves of these algorithms are showed in Figure 1. When the oracle rewards are provided in Pusher and Reacher, our method outperforms PETS and MBPO: it converges more quickly with similar performance at convergence in Pusher, while in Reacher, not only does it learn faster but also performs better at convergence. As we use the same planning method (MPC) as PETS, results indicate that our model better captures uncertainty, which is beneficial to improving sample efficiency. When exploring in environments where both rewards and transition are unknown, our method learns significantly faster than previous model-based and model-free methods which do no require oracle rewards. Meanwhile, it matches the performance of SAC at convergence. Moreover, the performances of our algorithm in environments with and without oracle rewards can be similar, or even faster convergence (see Pusher with and without rewards), indicating that our algorithm excels at exploring both rewards and transitions.

From experimental results, it can be verified that our algorithm better captures the model uncertainty, and makes better use of uncertainty using posterior sampling. In our methods, by sampling from a Bayesian linear regression on a fitted feature space, and optimizing under the same sampled MDP in the whole episode instead of re-sampling at every step, the performance of our algorithm is guaranteed from a Bayesian view as analysed in Section 4. While PETS and MBPO use bootstrap ensembles of models with a limited ensemble size to "simulate" a Bayesian model, in which the convergence of the uncertainty is not guaranteed and is highly dependent on the training of the neural network. However, in our method there is a limitation of using MPC, which might fail in even higher-dimensional tasks shown in Janner et al. (2019). Incorporating policy gradient techniques for action-selection might further improve the performance and we leave it for future work.

7 Conclusion

In our paper, we derive a novel Bayesian regret for PSRL algorithm in continuous spaces with the assumption that true rewards and transitions (with or without feature embedding) can be modeled by GP with linear kernels. While matching the best-known bounds in previous works from a Bayesian view, PSRL also enjoys computational tractability. Moreover, we propose MPC-PSRL in continuous environments, and experiments show that our algorithm exceeds existing model-based and model-free methods with more efficient exploration.

REFERENCES

Mohammad Gheshlaghi Azar, Ian Osband, and Rémi Munos. Minimax regret bounds for reinforcement learning. *arXiv preprint arXiv:1703.05449*, 2017.

Kamyar Azizzadenesheli, Emma Brunskill, and Animashree Anandkumar. Efficient exploration through bayesian deep q-networks. In *2018 Information Theory and Applications Workshop (ITA)*, pp. 1–9. IEEE, 2018.

Gabriel Barth-Maron, Matthew W Hoffman, David Budden, Will Dabney, Dan Horgan, Dhruva Tb, Alistair Muldal, Nicolas Heess, and Timothy Lillicrap. Distributed distributional deterministic policy gradients. *arXiv preprint arXiv:1804.08617*, 2018.

Zdravko I Botev, Dirk P Kroese, Reuven Y Rubinstein, and Pierre L'Ecuyer. The cross-entropy method for optimization. In *Handbook of statistics*, volume 31, pp. 35–59. Elsevier, 2013.

Eduardo F Camacho and Carlos Bordons Alba. *Model predictive control*. Springer Science & Business Media, 2013.

Sayak Ray Chowdhury and Aditya Gopalan. Online learning in kernelized markov decision processes. In *The 22nd International Conference on Artificial Intelligence and Statistics*, pp. 3197–3205, 2019.

Kurtland Chua, Roberto Calandra, Rowan McAllister, and Sergey Levine. Deep reinforcement learning in a handful of trials using probabilistic dynamics models. In *Advances in Neural Information Processing Systems*, pp. 4754–4765, 2018.

Marc Deisenroth and Carl E Rasmussen. Pilco: A model-based and data-efficient approach to policy search. In *Proceedings of the 28th International Conference on machine learning (ICML-11)*, pp. 465–472, 2011.

Yarin Gal, Rowan McAllister, and Carl Edward Rasmussen. Improving pilco with bayesian neural network dynamics models. In *Data-Efficient Machine Learning workshop, ICML*, volume 4, pp. 34, 2016.

Tuomas Haarnoja, Aurick Zhou, Pieter Abbeel, and Sergey Levine. Soft actor-critic: Off-policy maximum entropy deep reinforcement learning with a stochastic actor. *arXiv preprint arXiv:1801.01290*, 2018.

Thomas Jaksch, Ronald Ortner, and Peter Auer. Near-optimal regret bounds for reinforcement learning. *Journal of Machine Learning Research*, 11(Apr):1563–1600, 2010.

Michael Janner, Justin Fu, Marvin Zhang, and Sergey Levine. When to trust your model: Model-based policy optimization. In *Advances in Neural Information Processing Systems*, pp. 12498–12509, 2019.

Chi Jin, Zeyuan Allen-Zhu, Sebastien Bubeck, and Michael I Jordan. Is q-learning provably efficient? In *Advances in Neural Information Processing Systems*, pp. 4863–4873, 2018.

Chi Jin, Zhuoran Yang, Zhaoran Wang, and Michael I Jordan. Provably efficient reinforcement learning with linear function approximation. In *Conference on Learning Theory*, pp. 2137–2143, 2020.

Sanket Kamthe and Marc Deisenroth. Data-efficient reinforcement learning with probabilistic model predictive control. In *International Conference on Artificial Intelligence and Statistics*, pp. 1701–1710. PMLR, 2018.

Ian Osband and Benjamin Van Roy. Model-based reinforcement learning and the eluder dimension. In *Advances in Neural Information Processing Systems*, pp. 1466–1474, 2014.

Ian Osband and Benjamin Van Roy. Why is posterior sampling better than optimism for reinforcement learning? In Doina Precup and Yee Whye Teh (eds.), *Proceedings of the 34th International Conference on Machine Learning*, pp. 2701–2710, International Convention Centre, Sydney, Australia, 2017. PMLR.

Ian Osband, Van Roy Benjamin, and Russo Daniel. (More) efficient reinforcement learning via posterior sampling. In *Proceedings of the 26th International Conference on Neural Information Processing Systems - Volume 2*, NIPS'13, pp. 3003–3011, USA, 2013. Curran Associates Inc.

Ian Osband, Benjamin Van Roy, Daniel J Russo, and Zheng Wen. Deep exploration via randomized value functions. *Journal of Machine Learning Research*, 20(124):1–62, 2019.

Carl Edward Rasmussen. Gaussian processes in machine learning. In *Summer School on Machine Learning*, pp. 63–71. Springer, 2003.

Phillippe Rigollet and Jan-Christian Hütter. High dimensional statistics. *Lecture notes for course 18S997*, 2015.

Carlos Riquelme, George Tucker, and Jasper Snoek. Deep bayesian bandits showdown: An empirical comparison of bayesian deep networks for thompson sampling. *arXiv preprint arXiv:1802.09127*, 2018.

Daniel Russo and Benjamin Van Roy. Learning to optimize via posterior sampling. *Mathematics of Operations Research*, 39(4):1221–1243, 2014.

Niranjan Srinivas, Andreas Krause, Sham M Kakade, and Matthias W Seeger. Information-theoretic regret bounds for gaussian process optimization in the bandit setting. *IEEE Transactions on Information Theory*, 58(5):3250–3265, 2012.

William R Thompson. On the likelihood that one unknown probability exceeds another in view of the evidence of two samples. *Biometrika*, 25(3/4):285–294, 1933.

Christopher KI Williams and Francesco Vivarelli. Upper and lower bounds on the learning curve for gaussian processes. *Machine Learning*, 40(1):77–102, 2000.

Lin F Yang and Mengdi Wang. Reinforcement learning in feature space: Matrix bandit, kernels, and regret bound. *arXiv preprint arXiv:1905.10389*, 2019.

Andrea Zanette, Alessandro Lazaric, Mykel Kochenderfer, and Emma Brunskill. Learning near optimal policies with low inherent bellman error. *arXiv preprint arXiv:2003.00153*, 2020.

A Appendix

A.1 Proof of Lemma 1

Here we provide a proof of Lemma 1.

We first prove the results in $\mathbb{R}^d$ with $d = 1$: $p_1(x) \sim \mathcal{N}(\mu, \sigma^2), p_2(x) \sim \mathcal{N}(\mu', \sigma^2)$, without loss of generality, assume $\mu' \geq \mu$. The probabilistic distribution is symmetric with regard to $\frac{\mu+\mu'}{2}$. Note that $p_1(x) = p_2(x)$ at $x = \frac{\mu+\mu'}{2}$. Thus the integration of absolute difference between pdf of p_1 and p_2 can be simplified as twice the integration of one side:

$$\int_{-\infty}^{\infty} |p_2(x) - p_1(x)| dx = \frac{2}{\sqrt{2\pi\sigma^2}} \int_{\frac{\mu+\mu'}{2}}^{\infty} e^{\frac{-(x-\mu')^2}{2\sigma^2}} - e^{\frac{-(x-\mu)^2}{2\sigma^2}} dx \tag{11}$$

let $z_1 = x - \mu$, $z_2 = x - \mu'$, we have:

$$\begin{aligned}
&\frac{2}{\sqrt{2\pi\sigma^2}} \int_{\frac{\mu+\mu'}{2}}^{\infty} e^{\frac{-(x-\mu')^2}{2\sigma^2}} - e^{\frac{-(x-\mu)^2}{2\sigma^2}} dx \\
&= \sqrt{\frac{2}{\pi\sigma^2}} \int_{\frac{\mu-\mu'}{2}}^{\infty} e^{-\frac{z_2^2}{2\sigma^2}} dz_2 - \sqrt{\frac{2}{\pi\sigma^2}} \int_{\frac{\mu'-\mu}{2}}^{\infty} e^{-\frac{z_1^2}{2\sigma^2}} dz_1 \\
&= \sqrt{\frac{2}{\pi\sigma^2}} \int_{\frac{\mu'-\mu}{2}}^{\frac{\mu'-\mu}{2}} e^{-\frac{z^2}{2\sigma^2}} dz \\
&= 2\sqrt{\frac{2}{\pi\sigma^2}} \int_{0}^{\frac{\mu'-\mu}{2}} e^{-\frac{z^2}{2\sigma^2}} dz \leq 2\sqrt{\frac{2}{\pi\sigma^2}} \int_{0}^{\frac{\mu'-\mu}{2}} 1 dz = \sqrt{\frac{2}{\pi\sigma^2}} |\mu' - \mu|.
\end{aligned} \tag{12}$$

Now we extend the result to $\mathbb{R}^d (d \geq 2)$: $p_1(x) \sim \mathcal{N}(\mu, \sigma^2 I), p_2(x) \sim \mathcal{N}(\mu', \sigma^2 I)$. We can rotate the coordinate system recursively to align the last axis with vector $\mu - \mu'$, such that the coordinates of μ and μ' can be written as $(0, 0, \cdots, 0, \hat{\mu})$, and $(0, 0, \cdots, 0, \hat{\mu}')$ respectively, with $|\hat{\mu}' - \hat{\mu}| = \|\mu - \mu'\|_2$. Without loss of generality, let $\hat{\mu} \geq \hat{\mu}'$.

Clearly, all points with equal distance to $\hat{\mu}'$ and $\hat{\mu}$ define a hyperplane $P : x_d = \frac{\hat{\mu}+\hat{\mu}'}{2}$ where $p_1(x) = p_2(x), \forall x \in P$. More specifically, the probabilistic distribution is symmetric with regard to P. Similar to the analysis in $\mathbb{R}^1$:

$$
\begin{aligned}
&\int_{-\infty}^{\infty}\int_{-\infty}^{\infty}\cdots\int_{-\infty}^{\infty}|p_1(x)-p_2(x)|dx_1dx_2\cdots dx_d \\
&= \frac{2}{\sqrt{(2\pi)^d\sigma^{2d}}}\int_{-\infty}^{\infty}\int_{-\infty}^{\infty}\cdots\int_{\frac{\hat{\mu}+\hat{\mu}'}{2}}^{\infty} e^{\frac{-x_1^2}{2\sigma^2}}\cdots e^{\frac{-x_{d-1}^2}{2\sigma^2}} e^{\frac{-(x_d-\hat{\mu})^2}{2\sigma^2}} dx_1dx_2\cdots dx_d \\
&- \frac{2}{\sqrt{(2\pi)^d\sigma^{2d}}}\int_{-\infty}^{\infty}\int_{-\infty}^{\infty}\cdots\int_{\frac{\hat{\mu}+\hat{\mu}'}{2}}^{\infty} e^{\frac{-x_1^2}{2\sigma^2}}\cdots e^{\frac{-x_{d-1}^2}{2\sigma^2}} e^{\frac{-(x_d-\hat{\mu}')^2}{2\sigma^2}} dx_1dx_2\cdots dx_d \\
&= \frac{2}{\sqrt{(2\pi)^d\sigma^{2d}}}\int_{-\infty}^{\infty} e^{\frac{-x_1^2}{2\sigma^2}}dx_1\int_{-\infty}^{\infty} e^{\frac{-x_2^2}{2\sigma^2}}dx_2\cdots\int_{-\infty}^{\infty} e^{\frac{-x_{d-1}^2}{2\sigma^2}}dx_{d-1}\int_{\frac{\hat{\mu}+\hat{\mu}'}{2}}^{\infty} e^{\frac{-(x_d-\hat{\mu})^2}{2\sigma^2}}dx_d \\
&- \frac{2}{\sqrt{(2\pi)^d\sigma^{2d}}}\int_{-\infty}^{\infty} e^{\frac{-x_1^2}{2\sigma^2}}dx_1\int_{-\infty}^{\infty} e^{\frac{-x_2^2}{2\sigma^2}}dx_2\cdots\int_{-\infty}^{\infty} e^{\frac{-x_{d-1}^2}{2\sigma^2}}dx_{d-1}\int_{\frac{\hat{\mu}+\hat{\mu}'}{2}}^{\infty} e^{\frac{-(x_d-\hat{\mu}')^2}{2\sigma^2}}dx_d \\
&= \sqrt{\frac{2}{\pi\sigma^2}}\left(\int_{\frac{\hat{\mu}+\hat{\mu}'}{2}}^{\infty} e^{\frac{-(x_d-\hat{\mu})^2}{2\sigma^2}}dx_d - \int_{\frac{\hat{\mu}+\hat{\mu}'}{2}}^{\infty} e^{\frac{-(x_d-\hat{\mu}')^2}{2\sigma^2}}dx_d\right)
\end{aligned}
\tag{13}
$$

let $z_1 = x_d - \hat{\mu}$,$z_2 = x_d - \hat{\mu}'$, we have:

$$
\begin{aligned}
&\int_{\frac{\hat{\mu}+\hat{\mu}'}{2}}^{\infty} e^{\frac{-(x_d-\hat{\mu})^2}{2\sigma^2}}dx_d - \int_{\frac{\hat{\mu}+\hat{\mu}'}{2}}^{\infty} e^{\frac{-(x_d-\hat{\mu}')^2}{2\sigma^2}}dx_d \\
&= \int_{\frac{\hat{\mu}'-\hat{\mu}}{2}}^{\infty} e^{\frac{-z_1^2}{2\sigma^2}}dz_1 - \int_{\frac{\hat{\mu}-\hat{\mu}'}{2}}^{\infty} e^{\frac{-z_2^2}{2\sigma^2}}dz_2 \\
&= \int_{\frac{\hat{\mu}'-\hat{\mu}}{2}}^{\frac{\hat{\mu}-\hat{\mu}'}{2}} e^{\frac{-z_2}{2\sigma^2}}dz \\
&= 2\int_{0}^{\frac{\hat{\mu}-\hat{\mu}'}{2}} e^{\frac{-z_2}{2\sigma}}dz \leq 2\int_{0}^{\frac{\hat{\mu}-\hat{\mu}'}{2}} 1dz \\
&= |\hat{\mu}-\hat{\mu}'|
\end{aligned}
\tag{14}
$$

Thus $\int_{-\infty}^{\infty}\int_{-\infty}^{\infty}\cdots\int_{-\infty}^{\infty}|p_1(x)-p_2(x)|dx_1dx_2\cdots dx_d \leq \sqrt{\frac{2}{\pi\sigma^2}}\,\|\mu-\mu'\|_2$.

A.2 Experimental details

Here we provide hyperparameters for MBPO:

env	cartpole	pendulum	pusher	reacher
env steps per episode	200	200	150	150
model rollouts per env step	400			
ensemble size	5			
network architecture	MLP with 2 hidden layers of size 200	MLP with 2 hidden layers of size 200	MLP with 4 hidden layers of size 200	MLP with 4 hidden layers of size 200
policy updates per env step	40			
model horizon	1->15 from episode 1->30	1->15 from episode 1->30	1	1->15 from episode 1->30

Table 1: Hyperparamters for MBPO

And we provide hyperparamters for MPC and Neural Networks in PETS:

env	pusher	reacher
env steps per episode	150	150
popsize	500	400
number of elites	50	50
network architecture	MLP with 4 hidden layers of size 200	
planning horizon	30	30
max iter	5	
ensemble size	5	

Table 2: Hyperparamters for PETS

Here are hyperparameters of our algorithm, which is similar with PETS, except for ensemble size(since we do not use ensembled models):

env	cartpole	pendulum	pusher	reacher
env steps per episode	200	200	150	150
popsize	500	100	500	400
number of elites	50	5	50	50
network architecture	MLP with 2 hidden layers of size 200	MLP with 2 hidden layers of size 200	MLP with 4 hidden layers of size 200	MLP with 4 hidden layers of size 200
planning horizon	30	20	30	30
max iter	5			

Table 3: Hyperparamters for our method

For SAC and DDPG, we use the open source code (`https://github.com/dongminlee94/deep_rl`) for implementation without changing their hyperparameters. Here we thank the author for sharing the code!